

# DIVERSE VARIABILITY OF O AND B STARS REVEALED FROM 2-MINUTE CADENCE LIGHT CURVES IN SECTORS 1 AND 2 OF THE TESS MISSION: SELECTION OF AN ASTEROSEISMIC SAMPLE

MAY G. PEDERSEN,<sup>1</sup> SOWGATA CHOWDHURY,<sup>2</sup> COLE JOHNSTON,<sup>1</sup> DOMINIC M. BOWMAN,<sup>1</sup> CONNY AERTS,<sup>1,3</sup>  
GERALD HANDLER,<sup>2</sup> PETER DE CAT,<sup>4</sup> CORALIE NEINER,<sup>5</sup> ALEXANDRE DAVID-URAZ,<sup>6</sup> DEREK BUZASI,<sup>7</sup>  
ANDREW TKACHENKO,<sup>1</sup> SERGIO SIMÓN-DÍAZ,<sup>8</sup> EHSAN MORAVVEJI,<sup>1</sup> JAMES SIKORA,<sup>9</sup> GIOVANNI M. MIROUH,<sup>10</sup>  
CATHERINE C. LOVEKIN,<sup>11</sup> MATTEO CANTIELLO,<sup>12,13</sup> JADWIGA DASZYŃSKA-DASZKIEWICZ,<sup>14</sup> ANDRZEJ PIGULSKI,<sup>14</sup>  
ROLAND K. VANDERSPEK,<sup>15</sup> AND GEORGE R. RICKER<sup>15</sup>

<sup>1</sup>*Instituut voor Sterrenkunde, KU Leuven, Celestijnenlaan 200D, 3001 Leuven, Belgium*

<sup>2</sup>*Nicolaus Copernicus Astronomical Center, Bartycka 18, 00-716 Warszawa, Poland*

<sup>3</sup>*Department of Astrophysics, IMAPP, Radboud University Nijmegen, PO Box 9010, NL-6500 GL Nijmegen, the Netherlands*

<sup>4</sup>*Royal Observatory of Belgium, Ringlaan 3, 1180 Brussel, Belgium*

<sup>5</sup>*LESIA, Paris Observatory, PSL University, CNRS, Sorbonne Université, Univ. Paris Diderot, Sorbonne Paris Cité, 5 place Jules Janssen, 92195 Meudon, France*

<sup>6</sup>*Department of Physics and Astronomy, University of Delaware, Newark, DE 19716, USA*

<sup>7</sup>*Dept. of Chemistry & Physics, Florida Gulf Coast University, 10501 FGCU Blvd. S., Fort Myers, FL 33965 USA*

<sup>8</sup>*(Instituto de Astrofísica de Canarias, 38200 La Laguna, Tenerife, Spain*

<sup>9</sup>*Department of Physics, Engineering Physics and Astronomy, Queens University, Kingston, ON K7L 3N6 Canada*

<sup>10</sup>*Astrophysics Research Group, Faculty of Engineering and Physical Sciences, University of Surrey, Guildford GU2 7XH, UK*

<sup>11</sup>*Physics Department, Mount Allison University, Sackville, NB, E4L 1C6, Canada*

<sup>12</sup>*Center for Computational Astrophysics, Flatiron Institute, 162 5th Avenue, New York, NY 10010, USA*

<sup>13</sup>*Department of Astrophysical Sciences, Princeton University, Princeton, NJ 08544, USA*

<sup>14</sup>*Instytut Astronomiczny, Uniwersytet Wrocławski, Kopernika 11, 51-611 Wrocław, Poland*

<sup>15</sup>*Department of Physics, and Kavli Institute for Astrophysics and Space Research, Massachusetts Institute of Technology, Cambridge, MA 02139, USA*

(Received XXXX; Revised YYYY; Accepted ZZZZ)

Submitted to ApJL

## ABSTRACT

Uncertainties in stellar structure and evolution theory are largest for stars undergoing core convection on the main sequence. A powerful way to calibrate the free parameters used in the theory of stellar interiors is asteroseismology, which provides direct measurements of angular momentum and element transport. We report the detection and classification of new variable O and B stars using high-precision short-cadence (2-min) photometric observations assembled by the *Transiting Exoplanet Survey Satellite* (TESS). In our sample of 154 O and B stars, we detect a high percentage (90%) of variability. Among these we find 23 multiperiodic pulsators, 6 eclipsing binaries, 21 rotational variables, and 25 stars with stochastic low-frequency variability. Several additional variables overlap between these categories. Our study of O and B stars not only demonstrates the high data quality achieved by TESS for optimal studies of the variability of the most massive stars in the Universe, but also represents the first step towards the selection and composition of a large sample of O and B pulsators with high potential for joint asteroseismic and spectroscopic modeling of their interior structure with unprecedented precision.

*Keywords:* asteroseismology — stars: massive — stars: evolution — stars: oscillations — stars: rotation — binaries: general

## 1. INTRODUCTION

The variability of stars born with a mass  $M \geq 3M_{\odot}$  is diverse in terms of periodicity (minutes to centuries)

and amplitude ( $\mu\text{mag}$  to  $\text{mag}$ , see e.g. [Aerts et al. 2010](#)). Here, we are concerned with dwarfs, giants, and supergiants, of spectral type O or B. Such stars have a high binarity rate, a phenomenon that cannot be ignored when testing stellar evolution theory ([Sana et al. 2014](#); [Almeida et al. 2017](#); [Schneider et al. 2018](#)). Throughout their life, these stars are also subject to a strong variable radiation-driven wind (e.g. [Lucy & Solomon 1970](#); [Castor et al. 1975](#); [Owocki & Rybicki 1984](#); [Krtićka & Feldmeier 2018](#)).

Compared to other classes of variables, O stars have hardly been monitored with high-precision long-duration space photometry – see Table 3 in [Buysschaert et al. \(2015\)](#) for a summary of space photometric time-series studies of O stars, and more recent studies of their descendants including [Pablo et al. \(2017\)](#); [Johnston et al. \(2017\)](#); [Buysschaert et al. \(2017b\)](#); [Aerts et al. \(2018a\)](#); [Simón-Díaz et al. \(2018\)](#); [Ramiamanantsoa et al. \(2018a,b\)](#). Aside from single and multiperiodic pulsational, binary and rotational variability, these studies also revealed stochastic low-frequency variability. This observed phenomenon was interpreted in terms of internal gravity waves (IGWs) by [Aerts & Rogers \(2015\)](#). The observational signatures of IGWs have meanwhile been investigated systematically from CoRoT and K2 data by [Bowman et al. \(2018\)](#) and [Bowman et al. \(submitted\)](#), respectively. They offer an entirely new way of asteroseismic investigation by bridging 3D hydrodynamical simulations of stochastically excited waves and 1D theory of stellar interiors ([Aerts et al. 2019](#), Fig. 1).

Classical gravity-mode asteroseismology, i.e., forward modeling of the frequencies of coherent identified gravity modes (see [Aerts et al. 2018b](#), for the methodology), has so far been limited to some 40 stars of spectral type B or F, covering the mass range  $M \in [1.3, 8] M_{\odot}$  and rotation rates from almost zero up to 80% of critical breakup. This revealed the capacity of high-precision ( $\sim 10\%$ ) mass estimation of single stars (see [Moravveji et al. 2015, 2016](#); [Szewczuk & Daszyńska-Daszkiewicz 2018](#), for B stars and [Mombarg et al. \(submitted\)](#) for F stars) and of binaries ([Kallinger et al. 2017](#); [Johnston et al. 2019](#)). So far, these asteroseismic studies using space photometry revealed almost rigid rotation for the stars whose near-core ( $\Omega_{\text{core}}$ ) and envelope ( $\Omega_{\text{env}}$ ) rotation could be estimated, following the few earlier results of  $\Omega_{\text{core}}/\Omega_{\text{env}} \in [1, 5]$  from ground-based asteroseismology of early-B stars (see [Aerts 2015](#), for a summary). These asteroseismic findings challenge current angular momentum transport theories across the entire mass range ([Aerts et al. 2019](#)).

This *Letter* introduces our dedicated study to investigate single and binary O and B stars with the NASA *Transiting Exoplanet Survey Satellite* (TESS) mission ([Ricker et al. 2015](#)). In order to perform asteroseismology, one first needs to find suitable multiperiodic O and B pulsators. We achieve this by classifying the variability of 154 O and B stars observed in and proposed for short cadence mode by the *TESS Asteroseismic Science Consortium* (TASC). We present our classification and selection strategy for the 2-min cadence light curves obtained in Sectors 1 and 2 of the TESS mission.

## 2. METHOD

### 2.1. TESS light curve extraction

To study the variability of massive stars, we analyse a sample of 154 O and B stars observed by TESS with 2-min cadence, of which 40 are located in the Large Magellanic Cloud (LMC). These 154 stars were identified as O and B stars based on the spectral types provided in SIMBAD<sup>1</sup>. The data treated here were obtained by TESS in Sectors 1 (July 25 – August 22, 2018) and 2 (August 23 – September 20, 2018) and are publicly available via the Mikulski Archive for Space Telescopes (MAST)<sup>2</sup>. The extracted time series are in the format of reduced Barycentric Julian Date (BJD – 2457000) and stellar magnitudes, where the latter have been adjusted to show variability around zero by subtracting the mean. Where necessary, we performed detrending of long-term instrumental effects by means of subtracting a linear or low-order polynomial fit.

### 2.2. Classification procedure

We calculated amplitude spectra of all light curves using Discrete Fourier Transforms (DFT) following the method by [Kurtz \(1985\)](#). We used an oversampling factor of ten to ensure that all frequency peaks in the DFT are adequately sampled. The 2-min cadence of TESS results in a Nyquist frequency of  $360 \text{ d}^{-1}$ , which is sufficiently high to avoid a bias when extracting significant frequencies using iterative prewhitening. Amplitude suppression of variability in time series is negligible within the frequency range of interest for such high sampling ([Bowman 2017](#)). Based on visual inspection of the light curves and amplitude spectra by several of the authors independently, we provide the variability classification of all 154 O and B stars in Table 1 in Appendix A. We also report the number of available échelle spectra in the public ESO archive<sup>3</sup> for each of the stars and the

<sup>1</sup> <http://simbad.u-strasbg.fr/simbad/>

<sup>2</sup> [http://archive.stsci.edu/tess/all\\_products.html](http://archive.stsci.edu/tess/all_products.html)

<sup>3</sup> [http://archive.eso.org/eso/eso\\_archive\\_main.html](http://archive.eso.org/eso/eso_archive_main.html)

instrument used for the observations. This information is relevant for future studies of these 154 O and B stars. Figures of the light curves and amplitude spectra are made available electronically in Appendix B.

### 2.3. *Gaia* color-magnitude diagram

Asteroseismic modeling of stars with coherent oscillation modes can be optimally performed if at least one additional global stellar parameter (aside from the identified oscillation frequencies) can be measured with high precision. The availability of such an independent measurement helps to break degeneracies among the global and local stellar model parameters to be estimated (e.g., [Moravveji et al. 2015](#), Figs 5 and B.1). A model-independent mass from binarity ([Johnston et al. 2019](#)) or a high-precision (10%) spectroscopic estimate of the effective temperature ([Mombarg et al.](#), submitted) have been used to break degeneracies. Another useful quantity is a star’s luminosity ([Pedersen et al.](#), in preparation).

With this in mind, and to check the SIMBAD spectral types that went into the selection of our sample, we used *Gaia* DR2 photometry ([Gaia Collaboration et al. 2018a](#)) to place all sample stars in a color-magnitude diagram (CMD, Fig. 1). Each star was color-coded by its dominant variability type. The apparent *Gaia* G-band magnitudes were converted to absolute magnitudes  $M_G$  using the *Gaia* DR2 distances from [Bailer-Jones et al. \(2018\)](#). The colors were derived from the apparent *Gaia* BP and RP band magnitudes. All other stars observed in 2-min cadence by TESS in Sectors 1 and 2 with *Gaia* DR2 data available (20883 out of the 24816 TESS targets) were included as black dots. Using the same approach as in [Gaia Collaboration et al. \(2018b\)](#), the position of the stars in Fig. 1 have not been corrected for reddening or extinction, but we show a typical  $2\sigma$  error bar for the positioning of the stars in the CMD. Two stars (TIC 197641601 = HD 207971 and TIC 354671857 = HD 14228) are outliers in the CMD (at BP-RP > 2). Although these stars are B stars, they are very bright ( $V = 3.01$  and  $3.57$ , respectively), which explains the discrepant *Gaia* photometry.

The 151 out of 154 stars in our sample observed with *Gaia* shown in Fig. 1 constitute the first sample of variable O and B stars monitored at high cadence in high-precision space photometry, after the K2 sample monitored at 30-min cadence in [Bowman et al. \(submitted\)](#). These two samples, along with future ones assembled by the TESS mission, will reveal numerous O and B stars suitable for asteroseismic modeling. Such modeling requires a frequency precision better than  $0.001 \text{ d}^{-1}$  and pulsation mode identification for tens of modes ([Aerts](#)

[et al. 2018b](#)). In this way, we will extend the large *Kepler* samples of low-mass and intermediate-mass pulsators with estimation of their interior rotation profile discussed in [Aerts et al. \(2019\)](#) to higher masses. The interior rotation and chemical mixing profiles, will hence be calibrated asteroseismically for large samples of massive stars that will eventually explode as supernovae.

## 3. RESULTS

It is not possible to discuss each star in the sample individually. Here we focus on the binarity and pulsational properties, and briefly discuss the detection of rotational and/or magnetic properties of the sample. Out of 154 stars, 41 show clear variability in their light curves but their nature could not yet be uniquely identified. These stars are marked by open black circles in Fig. 1.

### 3.1. *Eclipsing binaries*

Eclipsing binaries (EBs) hold the potential to provide model-independent distance, radius, and mass estimates and are crucial calibrators for stellar evolution theory ([Torres et al. 2010](#), for a review). Unfortunately, the number of O and B stars in EBs observed with high-precision space photometry remains small compared to the thousands of binaries with low-mass components ([Kirk et al. 2016](#)).

Six of the stars in our sample were already known as EBs and we confirm this classification using the TESS data: HD 6882 ( $\zeta$  Phe), HD 61644 (V455 Car), HD 224113 (AL Scl), HD 42933 ( $\delta$  Pic), HD 31407 (AN Dor), and HD 46792 (AE Pic). Their light curves in Appendix B are of unprecedented quality and future modeling will improve their mass determinations. One of these stars (HD 42933) is known to have  $\beta$  Cep type pulsations detected from BRITe photometry ([Pigulski et al. 2017](#)). We confirm the variability. In addition, three objects (HD 224990, HD 269382 and HD 53921) were known spectroscopic binaries, while ten more (HD 269676, HD 68520, HD 19400, HD 53921, HD 2884, HD 46860, HD 208433, HD 37854, HD 209014 and CPD-60 944) were listed as double or multiple stars in SIMBAD; the TESS light curves of these 13 non-eclipsing binaries did not show traces of the binary nature. The only exception is HD 208433, which shows a single transit. In addition, we find four showing either ellipsoidal variation or rotational modulation: HD 268798, HD 222847, HD 20784 and HD 37935. None of these four stars have previously been identified as binaries, but HD 37935 is a known Be star.

HD 53921 is a known spectroscopic magnetic binary, which was identified as a Slowly Pulsating B (SPB) star by [De Cat & Aerts \(2002\)](#). From the high-quality

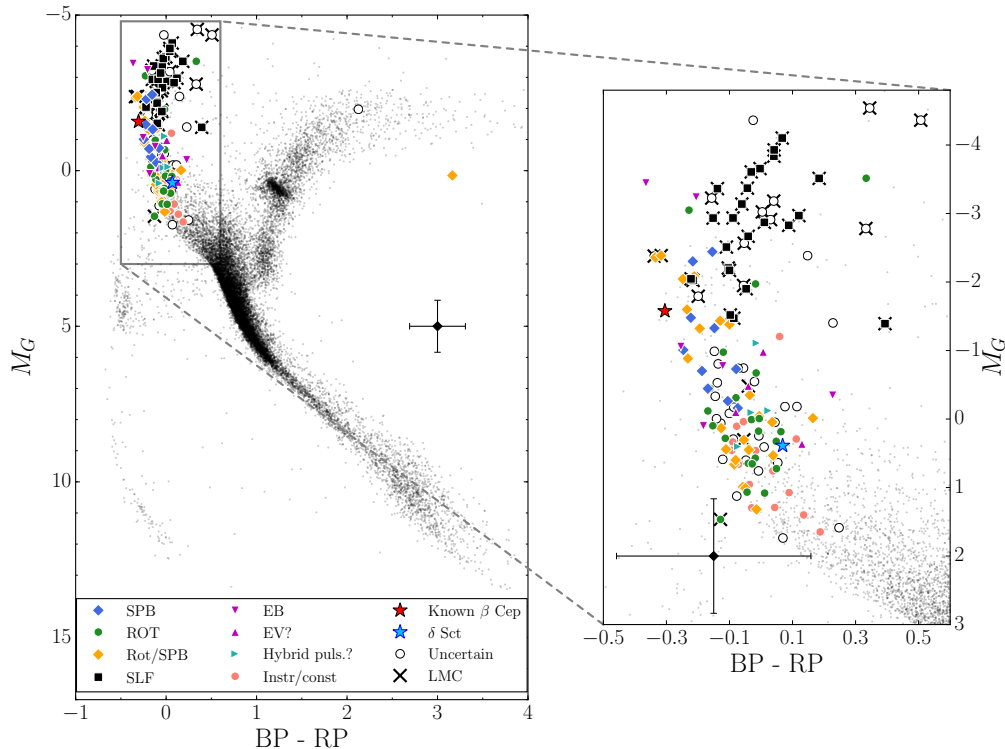


**Figure 1.** Classification results for O and B stars placed in a Gaia DR2 CMD. Black dots are the entire TESS sector 1 and 2 short-cadence stars also observed by Gaia, and open black circles corresponds to uncertain classification. The labels in the legend correspond to the following types of variability: SLF = Stochastic low-frequency signal, Instr/const = instrumental or constant, SPB = slowly pulsating B star, ROT = rotational modulation, ROT/SPB = rotational modulation and/or SPB, Hybrid puls.? = both p- and g-modes, EB = Eclipsing Binary, EV? = Ellipsoidal variable or rotational modulation,  $\delta$  Set =  $\delta$  Scuti star. The error bar shows a typical  $2\sigma$ -error on the position in the CMD, shown in both panels. LMC members are indicated by a  $\times$  behind their variability symbol.

TESS light curves we find that the dominant frequency of  $0.6054 \text{ d}^{-1}$  shows a second harmonic. Based on this as well as the morphology of the light curve, we deduce that this frequency is caused by rotational modulation. This example illustrates how difficult g-mode asteroseismology from ground-based observations can be. This and other known magnetic stars in the sample are discussed in detail in David-Uraz et al. (in prep.).

In total, eight of these 19 binaries reveal pulsations. We show the phased light curve for a newly discovered binary pulsator (HD 61644=TIC 349907707) in Fig. 2. This result illustrates the promise of TESS to provide numerous pulsating O and B binaries suitable to calibrate stellar evolution models from binary asteroseismology (Johnston et al. 2019).

### 3.2. Pulsating stars

Coherent non-radial oscillation modes in O and B stars come in two main flavors: pressure modes with periods of a few hours ( $\beta$  Cep stars, spectral types from O9 to B3) and gravity modes with periods of order a few days (SPB stars, spectral types from late O to B9).

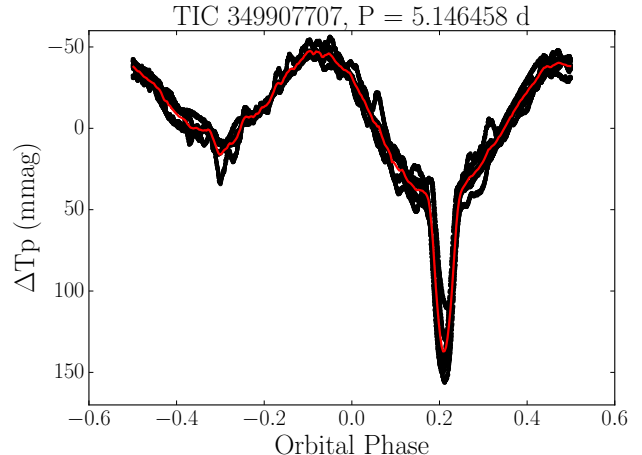


**Figure 2.** Phase folded light curve (black) of the known eclipsing binary HD 61644, showing the signature of pulsations. The red line shows the binned phase curve.

For a discussion on their early discoveries and pulsation properties, we refer to Aerts et al. (2010, Chapter 2). The space-based photometry assembled with MOST,

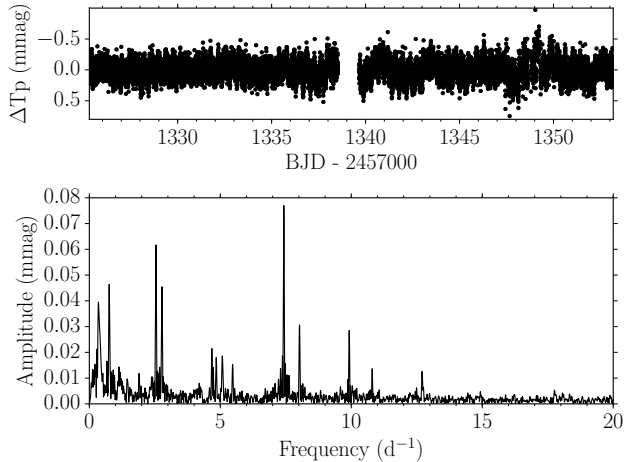


**Figure 3.** Example of a newly-discovered hybrid pulsator showing both SPB and  $\beta$  Cep type pulsations (TIC 469906369 = HD 212581). The TESS light curve and amplitude spectrum are shown in the top and bottom panels, respectively.

CoRoT, *Kepler*, K2, and BRIDE revealed that many O and B pulsators are *hybrids*, i.e., pulsators with both types of modes simultaneously. Such hybrid pulsators have proven to be a powerful tool for constraining opacities in the partial ionization layers responsible for the mode excitation. As an example, the detailed seismic modeling of  $\nu$  Eri performed by [Daszyńska-Daszkiewicz et al. \(2017\)](#) revealed that a factor three increase in the opacity at  $\log T = 5.46$  was needed to excite the g-modes in this star.

In total, we find 14 new O and B pulsators, among which 10 have gravity modes and four are potential hybrids. We show the light curve and DFT for one of the newly discovered hybrid stars in Fig. 3. One star in the sample, HN Aqr, is a known  $\beta$  Cep star and is discussed in [Handler et al. \(submitted\)](#). Future continued TESS and/or spectroscopic monitoring will be needed to assess the asteroseismic potential of these 14 pulsators in terms of frequency precision and mode identification.

### 3.3. Rotational variability

We classified 21 of the stars in our sample as rotational variables, one of which is labeled as a Wolf Rayet star in SIMBAD (HD 269582). Among these are three stars previously known to be magnetic: HD 223640 ([Bychkov et al. 2005; Sikora et al. 2018](#)) and HD 53921 ([Hubrig et al. 2006; Bagnulo et al. 2015](#)), as well as HD 65987 ([Bagnulo et al. 2015](#)). Rotational modulation is usually interpreted as due to temperature and/or chemical spots on the stellar surface caused by large-scale magnetic fields. We refer to the accompanying papers by [David-Uraz et al. \(in prep.\)](#) and [Balona et al. \(submit-](#)

ted) for an extensive discussion of the rotational modulation and magnetic properties of the sample.

The star HD 10144 (aka Achernar and  $\alpha$  Eri) is a Be star rotating at 95% of critical breakup, whose stellar disk has been imaged by interferometry ([Dalla Vedova et al. 2017](#)). We find its dominant frequency to be  $0.729 \text{ d}^{-1}$ . Also HD 214748, HD 209522, HD 33599, HD 19818, HD 221507, HD 46860, HD 37974, HD 53048, CD-56 152, HD 209014, HD 37935, HD 68423, HD 224686 and HD 66194 were known to be Be stars prior to our study. While HD 221507 is known as a Be star, recent studies have shown that it lacks emission and has a low  $v \sin i$  (e.g. [Arcos et al. 2017](#)).

In addition to the stars classified as rotational variables, we found 25 stars which show rotational modulation and/or SPB type variability. The simultaneous occurrence of rotation and pulsation frequencies in space photometry is not unusual, but there is only one case so far for which combined spectropolarimetric and asteroseismic modeling has been achieved: the hybrid magnetic  $\beta$  Cep/SPB star HD 43317 monitored by CoRoT ([Buysschaert et al. 2017a, 2018](#)). Our results are encouraging to expand the domain of magneto-asteroseismology.

### 3.4. Stochastic, low-frequency signatures

Stochastic, low-frequency (SLF) variability has been shown to be a common phenomenon in blue supergiants in both space-based photometry ([Bowman et al. 2018](#)) and spectroscopy ([Simón-Díaz et al. 2018](#)). Several theories may explain this variability, such as sub-surface convection, dynamical stellar winds and IGWs excited at the convective core boundary (see [Bowman et al. 2018](#), for a detailed discussion). In our sample of 154 O and B stars, we find 25 stars with SLF, all of which are classified as blue supergiants based on the spectral types from SIMBAD and occurring near the terminal age main sequence (TAMS). This is in agreement with the conclusions by [Bowman et al. \(submitted\)](#) from K2 photometry of such stars, and opens up an entirely new avenue of forward modeling of evolved OB stars at and beyond the TAMS to tune their angular momentum and element transport observationally.

### 3.5. Other types of variability

We found several stars with “outbursts” in their light curves (see Table 1 and Appendix B). Such outbursts may be connected with episodic mass loss, such as in Be stars, or flaring due to magnetic activity in low-mass stars. In some cases, the detected outbursts occur in various of the light curves at the same time and for the same duration. This signature is instrumental. For the

remainder of the targets, spectroscopic follow-up and a study of the pixel data is required to confirm that the outbursts are physical, rather than instrumental artefacts (Pedersen et al. 2017, Balona et al. submitted).

#### 4. DISCUSSION AND CONCLUSIONS

We presented variability classification for 154 stars with spectral type O or B that were monitored in short-cadence (2-min) by the TESS mission in its Sectors 1 and 2. We found 138 to be variable at the TESS detection threshold. This is a high percentage of variability (90%) given that the time base of each sector is only 27 d, preventing longer-period variables from being discovered. We placed the 151 out of 154 targets with a Gaia DR2 parallax in a CMD (Fig. 1).

Our variability classification had the main goal to start compiling a large unbiased sample of O and B stars for future asteroseismology. Stars with multiple individual frequencies of identified coherent standing modes and/or low-frequency stochastically excited IGWs are suitable of asteroseismic probing. We found 15 single and 8 binary O and B coherent pulsators (i.e., 15% of the monitored stars) and 25 stars with stochastic low-frequency signatures (16%). All of these 25 stars are located in the LMC and cover a higher mass regime than the galactic targets. Unlike coherent modes, IGW driven by the convective core are independent of an iron opacity bump and should thus also be excited in low-metallicity stars. However, the low-frequency signal could also be produced by subsurface convection, which is strongly metal dependent (Cantiello et al. 2009). For all of the variable OB stars, an extension of the TESS light curve monitoring is needed to provide the frequency precision required for detailed asteroseismic modeling. Our ini-

tial study reveals the major potential of the combined long-term (+1 year) TESS, Gaia, and spectroscopic all-sky monitoring as already outlined by Kollmeier et al. (2017).

*Acknowledgements:* This paper includes data collected by the TESS mission. Funding for the TESS mission is provided by the NASA Explorer Program. Funding for the TESS Asteroseismic Science Operations Centre is provided by the Danish National Research Foundation (Grant agreement no.: DNR106), ESA PRODEX (PEA 4000119301) and Stellar Astrophysics Centre (SAC) at Aarhus University. We thank the TESS and TASC/TASOC teams for their support of the present work. This research has made use of the SIMBAD database, operated at CDS, Strasbourg, France. Some of the data presented in this paper were obtained from the Mikulski Archive for Space Telescopes (MAST). STScI is operated by the Association of Universities for Research in Astronomy, Inc., under NASA contract NAS5-2655. We acknowledge the ESO Science Archive Facility. The research leading to these results received funding and/or support from: the European Research Council (ERC) under the European Union’s Horizon 2020 research and innovation program (grant agreement No. 670519: MAMSIE), the Research Foundation Flanders (FWO) under the grant agreement G0H5416N (ERC runner-up grant), the STFC consolidated grant ST/R000603/1, the Polish NCN grant (no. 2015/17/B/ST9/02082, 2015/18/A/ST9/00578 and 2016/21/B/ST9/01126), and the Natural Science and Engineering Research Council (NSERC) of Canada. The Flatiron Institute is supported by the Simons Foundation.

#### REFERENCES

- Aerts, C. 2015, in IAU Symposium, Vol. 307, New Windows on Massive Stars, ed. G. Meynet, C. Georgy, J. Groh, & P. Stee, 154–164
- Aerts, C., Christensen-Dalsgaard, J., & Kurtz, D. W. 2010, *Asteroseismology*, Astronomy and Astrophysics Library, Springer-Verlag, Heidelberg
- Aerts, C., Mathis, S., & Rogers, T. 2019, *ARA&A*, in press (arXiv:1809.07779)
- Aerts, C., & Rogers, T. M. 2015, *ApJL*, 806, L33
- Aerts, C., Bowman, D. M., Símón-Díaz, S., et al. 2018a, *MNRAS*, 476, 1234
- Aerts, C., Molenberghs, G., Michielsen, M., et al. 2018b, *ApJS*, 237, 15
- Almeida, L. A., Sana, H., Taylor, W., et al. 2017, *A&A*, 598, A84
- Arcos, C., Jones, C. E., Sigut, T. A. A., Kanaan, S., & Curé, M. 2017, *ApJ*, 842, 48
- Bagnulo, S., Fossati, L., Landstreet, J. D., & Izzo, C. 2015, *A&A*, 583, A115
- Bailer-Jones, C. A. L., Rybizki, J., Foesneau, M., Mantelet, G., & Andrae, R. 2018, *AJ*, 156, 58
- Bowman, D. M. 2017, *Amplitude Modulation of Pulsation Modes in Delta Scuti Stars*, doi:10.1007/978-3-319-66649-5
- Bowman, D. M., Aerts, C., Johnston, C., et al. 2018, *A&A*, in press (arXiv1811.08023)

- Buysschaert, B., Aerts, C., Bowman, D. M., et al. 2018, *A&A*, 616, A148
- Buysschaert, B., Neiner, C., Briquet, M., & Aerts, C. 2017a, *A&A*, 605, A104
- Buysschaert, B., Aerts, C., Bloemen, S., et al. 2015, *MNRAS*, 453, 89
- Buysschaert, B., Neiner, C., Richardson, N. D., et al. 2017b, *A&A*, 602, A91
- Bychkov, V. D., Bychkova, L. V., & Madej, J. 2005, *A&A*, 430, 1143
- Cantiello, M., Langer, N., Brott, I., et al. 2009, *A&A*, 499, 279
- Castor, J. I., Abbott, D. C., & Klein, R. I. 1975, *ApJ*, 195, 157
- Dalla Vedova, G., Millour, F., Domiciano de Souza, A., et al. 2017, *A&A*, 601, A118
- Daszyńska-Daszkiewicz, J., Pamyatnykh, A. A., Walczak, P., et al. 2017, *MNRAS*, 466, 2284
- De Cat, P., & Aerts, C. 2002, *A&A*, 393, 965
- Gaia Collaboration, Brown, A. G. A., Vallenari, A., et al. 2018a, *A&A*, 616, A1
- Gaia Collaboration, Eyer, L., Rimoldini, L., et al. 2018b, *A&A*, in press, arXiv:1804.09382
- Hubrig, S., North, P., Schöller, M., & Mathys, G. 2006, *Astronomische Nachrichten*, 327, 289
- Johnston, C., Buysschaert, B., Tkachenko, A., Aerts, C., & Neiner, C. 2017, *MNRAS*, 469, L118
- Johnston, C., Tkachenko, A., Aerts, C., et al. 2019, *MNRAS*, 482, 1231
- Kallinger, T., Weiss, W. W., Beck, P. G., et al. 2017, *A&A*, 603, A13
- Kirk, B., Conroy, K., Prša, A., et al. 2016, *AJ*, 151, 68
- Kollmeier, J. A., Zasowski, G., Rix, H.-W., et al. 2017, *SDSS-V White Paper* (arXiv:1711.03234)
- Krtićka, J., & Feldmeier, A. 2018, *A&A*, 617, A121
- Kurtz, D. W. 1985, *MNRAS*, 213, 773
- Lucy, L. B., & Solomon, P. M. 1970, *ApJ*, 159, 879
- Moravveji, E., Aerts, C., Pápics, P. I., Triana, S. A., & Vandoren, B. 2015, *A&A*, 580, A27
- Moravveji, E., Townsend, R. H. D., Aerts, C., & Mathis, S. 2016, *ApJ*, 823, 130
- Owocki, S. P., & Rybicki, G. B. 1984, *ApJ*, 284, 337
- Pablo, H., Richardson, N. D., Fuller, J., et al. 2017, *MNRAS*, 467, 2494
- Pedersen, M. G., Antoci, V., Korhonen, H., et al. 2017, *MNRAS*, 466, 3060
- Pigulski, A., Jerzykiewicz, M., Ratajczak, M., Michalska, G., & Zahajkiewicz, E. 2017, in *Second BRITE-Constellation Science Conference: Small satellites—big science*, Proceedings of the Polish Astronomical Society volume 5, pp.120-127, ed. K. Zwintz & E. Poretti, 120–127
- Ramiamananantsoa, T., Ratnasingam, R., Shenar, T., et al. 2018a, *MNRAS*, 480, 972
- Ramiamananantsoa, T., Moffat, A. F. J., Harmon, R., et al. 2018b, *MNRAS*, 473, 5532
- Ricker, G. R., Winn, J. N., Vanderspek, R., et al. 2015, *Journal of Astronomical Telescopes, Instruments, and Systems*, 1, 014003
- Sana, H., Le Bouquin, J.-B., Lacour, S., et al. 2014, *ApJS*, 215, 15
- Schneider, F. R. N., Sana, H., Evans, C. J., et al. 2018, *Science*, 359, 69
- Sikora, J., Wade, G. A., Power, J., & Neiner, C. 2018, *MNRAS*, arXiv:1811.05635
- Simón-Díaz, S., Aerts, C., Urbaneja, M. A., et al. 2018, *A&A*, 612, A40
- Szewczuk, W., & Daszyńska-Daszkiewicz, J. 2018, *MNRAS*, 478, 2243
- Torres, G., Andersen, J., & Giménez, A. 2010, *A&A Rv*, 18, 67

## APPENDIX

## A. VARIABILITY CLASSIFICATION

In Table 1, we provide the TESS Input Catalogue (TIC) and Gaia identification numbers, as well as Gaia magnitudes and colours, **SIMBAD** spectral types and the classification of the dominant source(s) of variability for each of the 154 O and B stars observed by TESS in sectors 1 and 2 at a 2-min cadence.

Table 1. Identification numbers, parameters and variability classification of the 154 O and B stars.

| TIC       | Name           | Sp. Type<br>SIMBAD | Gaia DR2 ID         | $M_G$<br>(mag) | BP - RP<br>(mag) | # Spectra | Instrument | Var. Type   |
|-----------|----------------|--------------------|---------------------|----------------|------------------|-----------|------------|---|
| 12359289  | HD 225119      | Apsi               | 2333119869770412288 | -0.98          | -0.12            | 1         | F          | rot   |
| 29990592  | HD 268623      | B2Ia               | 4657589254497529344 | -4.10          | 0.07             | 1         | F          | SLF   |
| 30110048  | HD 268653      | B3Ia               | 4765410903770283008 | -2.02          | -0.22            | 1         | F          | SLF   |
| 30268695  | HD 268809      | B1Ia               | 5290767631226220032 | -2.20          | -0.10            | 1         | F          | SLF   |
| 30275662  | Sk-66 27       | B3Ia               | 4661771801060664064 | -3.37          | -0.04            | 4         | U          | SLF   |
| 30275861  | [HT83] a1f     | O6V                | 4662155839823561216 | 1.47           | -0.13            | -         | -          | rot   |
| 30312676  | HD 268726      | B2Ia               | 4662153812635167488 | -2.87          | 0.01             | 2         | U          | SLF   |
| 30312711  | BI 42          | O8V                | -                   | -              | -                | -         | -          | SLF / rot / EB?   |
| 30317301  | HD 268798      | B2Ia               | 4661511422956353152 | -3.02          | 0.00             | -         | -          | EV / rot / SLF  |
| 30933383  | Sk-68 39       | B2.5Ia             | 4662153469001983104 | -2.97          | 0.12             | 2         | F          | SLF   |
| 31105740  | TYC 9161-925-1 | B0.5Ia             | 4655458160445111552 | -2.93          | -0.15            | 1/3       | F/U        | SLF   |
| 31181554  | HD 269050      | B0Ia               | 4661392533937464448 | -2.05          | -0.22            | 22/12     | X/U        | SLF   |
| 31867144  | HD 22252       | B8IV               | 4671120982756449664 | -1.11          | -0.01            | -         | -          | rot / SPB + $\beta$ Cep hybrid?                               |
| 33945685  | HD 223118      | B9.5V              | 2338752697903817216 | 1.29           | 0.04             | -         | -          | instr? ( $\nu_{\text{inst}} \simeq 2.8 \text{ d}^{-1}$ )/puls |
| 38602305  | HD 27657 AB    | B9IV               | 4676067719930656640 | 0.28           | -0.11            | -         | -          | rot   |
| 40343782  | HD 269101      | B3Iab              | 5288240197589081728 | -3.18          | 0.04             | -         | -          | SLF / SPB?  |
| 41331819  | HD 43107       | B8V                | 5282761464287879296 | 0.29           | -0.09            | 84/12     | X/U        | rot / outburst?   |
| 47296054  | HD 214748      | B8Ve               | 6622561673163632768 | -1.38          | -0.10            | 26        | U          | rot / SPB / Be  |
| 49687057  | HD 220787      | B3III              | 4657674745869490304 | -2.38          | 0.15             | 6/18      | F/X        | instr / binary?   |
| 53992511  | HD 209522      | B4IVe              | 2436569757731466112 | -2.04          | -0.25            | 3/18/1/15 | F/X/E/U    | rot / SPB / Be  |
| 55295028  | HD 33599       | B2Vpe              | 6619440159652409728 | -1.60          | -0.23            | 1         | F          | rot / SPB / Be  |
| 66497441  | HD 222847      | B9V                | 2391220091406075648 | -0.10          | -0.08            | 1/42      | F/U        | EV / rot? / SPB?  |
| 69925250  | V* HN Aqr      | B                  | 2402031280004432512 | -1.58          | -0.30            | 4         | U          | known $\beta$ Cep   |
| 89545031  | HD 223640      | A0VpSiSr           | 2390144081839340288 | 0.10           | -0.15            | 33        | U          | rot   |
| 92136299  | HD 222661 A    | B9V                | 2419885149815948416 | 0.99           | -0.06            | 28        | U          | SPB+Be-type mini-outbursts / rot                              |
| 115177591 | HD 201108      | B8IV/V             | 6775980889978989824 | -0.16          | -0.07            | -         | -          | SPB   |
| 139468902 | HD 213155      | B9.5V              | 6521195703338406272 | 1.01           | -0.05            | 1/63/1    | F/X/U      | rot / SPB?  |
| 141281495 | HD 37854       | B9/9.5V            | 4648666996817764736 | 0.57           | -0.02            | -         | -          | rot?  |

Table 1 continued

Table 1 (continued)

| TIC       | Name              | Sp. Type<br>SIMBAD | Gaia DR2 ID         | $M_G$<br>(mag) | BP - RP<br>(mag) | # Spectra | Instrument | Var. Type  |
|-----------|-------------------|--------------------|---------------------|----------------|------------------|-----------|------------|--|
| 149039372 | HD 34543          | B8V                | 4663645952980782848 | 0.30           | -0.05            | -         | -          | rot? / SPB?  |
| 149971754 | HD 41297          | B8Ib               | 548201113182765696  | -0.26          | -0.11            | -         | -          | SPB  |
| 150357404 | HD 45796          | B6V                | 5477233430220256384 | -0.44          | -0.17            | 1         | F          | SPB  |
| 150442264 | HD 46792          | B2V                | 4760693797025929344 | -3.24          | -0.21            | -         | -          | EB + puls/rot  |
| 152283270 | HD 208433         | B9.5V              | 6588214059487740672 | 0.25           | -0.01            | -         | -          | instr / binary(transit)                                  |
| 167045028 | HD 45527          | B9IV               | 5279546835885790720 | 0.01           | -0.03            | -         | -          | rot  |
| 167415960 | HD 48467          | B8/9V              | 5266733784509615616 | 0.11           | -0.08            | 1         | F          | const?   |
| 167523976 | HD 49193          | B2V                | 4660166788974686976 | -1.48          | -0.22            | -         | -          | SPB  |
| 176935619 | HD 49306          | B9.5/A0V           | 5280155179351701504 | 1.02           | -0.05            | -         | -          | instr? ( $\nu_{\text{inst}} \simeq 2.8 \text{ d}^{-1}$ ) |
| 176955379 | HD 49531          | B8/9Vn             | 5279020208473101056 | 0.45           | -0.04            | -         | -          | SPB / rot  |
| 177075997 | HD 51557          | B7III              | 5266581089830743296 | -0.99          | -0.15            | 1         | F          | instr / rot?   |
| 179308923 | HD 269382         | O9.5Ib             | 4657651857940816640 | -2.57          | -0.05            | -         | -          | SLF? / SPB?  |
| 179574710 | HD 271213         | BIIak              | 4661778810447390720 | -1.47          | -0.09            | -         | -          | SLF  |
| 179637387 | [OM95] LH 47-373A | BIIa               | 4651354886129065600 | -1.52          | -0.10            | -         | -          | SLF  |
| 179639066 | HD 269440         | BIIb               | 4658741370886084992 | -2.17          | -0.10            | 2         | F          | SLF  |
| 182909257 | HD 6783           | Ap Si              | 4635279171434162304 | 0.65           | -0.04            | -         | -          | rot  |
| 197641601 | HD 207971         | B8IV-Vs            | 6586825380598277248 | -1.97          | 2.13             | 22        | U          | instr / rot  |
| 206362352 | HD 223145         | B3V                | 5283754052709233920 | -2.30          | -0.22            | 1/3/302   | F/X/U      | SPB  |
| 206547467 | HD 210780         | B9.5/A0            | 6819470079550296960 | 1.74           | 0.07             | -         | -          | rot / const? / SPB?                                      |
| 207176480 | HD 19818          | B9/A0Vn(e)         | 4723685987980665088 | 1.59           | 0.25             | 3         | F          | SPB? / SLF? / Be   |
| 207235278 | HD 20784          | B9.5V              | 4733510055655723392 | -0.98          | 0.01             | -         | -          | EV / rot   |
| 220430912 | HD 31407          | B2/3V              | 6522301330997312128 | -1.06          | -0.25            | 84        | X          | EB + puls  |
| 224244458 | HD 221507         | B9.5IIpHgMnSi      | 6538585991555664128 | 0.59           | -0.12            | 3/30      | F/U        | rot + mini-outburst?                                     |
| 229013861 | HD 208674         | B9.5V              | 6612822091790516480 | 1.07           | -0.04            | -         | -          | rot  |
| 230981971 | HD 10144          | B6Vpe              | -                   | -              | -                | 217/270   | F/U        | rot / SPB? / Be  |
| 231122278 | HD 29994          | B8/9V              | 4656238611846958208 | 0.53           | 0.04             | -         | -          | rot / SPB?   |
| 238194921 | HD 24579          | B7III              | 4627113682690040576 | -0.35          | -0.04            | -         | -          | rot / SPB  |
| 259862349 | HD 16978          | B9Va               | 4695167130257150592 | 0.66           | -0.07            | 6/9/20    | F/X/U      | instr  |
| 260128701 | HD 42918          | B4V                | 5494534348761557888 | -1.01          | -0.25            | -         | -          | SPB  |
| 260131665 | HD 42933          | B1/2(III)n         | 5499415974230271488 | -3.45          | -0.36            | 4         | F          | EB + $\beta$ Cep   |

Table 1 continued

Table 1 (continued)

| TIC       | Name         | Sp. Type<br>SIMBAD | Gaia DR2 ID         | $M_G$<br>(mag) | BP - RP<br>(mag) | # Spectra | Instrument | Var. Type   |
|-----------|--------------|--------------------|---------------------|----------------|------------------|-----------|------------|---|
| 260368525 | HD 44937     | B9.5V              | 5494983804202264192 | -0.18          | 0.11             | -         | -          | SPB?  |
| 260540898 | HD 46212     | B8IV               | 5496276314480471040 | -0.55          | -0.02            | -         | -          | rot?  |
| 260640910 | HD 46860 AB  | B9IVn+A8V:p?       | 5482771807727582080 | -0.73          | -0.08            | 2         | F          | SPB/Be  |
| 260820871 | HD 218801    | B9.5V(n)           | 6381543153782126464 | 0.60           | -0.05            | -         | -          | rot / binary?   |
| 261205462 | HD 40953     | B9V                | 4623532264081294464 | 0.66           | -0.08            | 1         | F          | SPB / rot   |
| 262815962 | HD 218976 AB | B9.5/A0V           | 6500025053617700992 | 1.32           | -0.01            | -         | -          | rot / SPB?  |
| 270070443 | HD 198174    | B8II               | 6805364208656989696 | -0.31          | -0.08            | -         | -          | rot   |
| 270219259 | HD 209014 AB | B8/9V+B8/9         | 6617682865193265536 | -1.40          | 0.23             | 3         | F          | instr / $\beta$ Cep + outburst                          |
| 270557257 | HD 49835     | B9.5V              | 5211969859107211136 | 1.40           | 0.14             | -         | -          | instr ( $\nu_{\text{inst}} \simeq 2.8 \text{ d}^{-1}$ ) |
| 270622440 | HD 224112    | B8V                | 2314214110928211712 | -0.08          | -0.10            | 3         | F          | EB (contamination!)                                     |
| 270622446 | HD 224113    | B5/8               | 2314213698611350144 | -0.78          | -0.12            | 36/18     | F/X        | EB  |
| 271503441 | HD 2884 AB   | B8/A0              | 4900927434176620160 | 1.12           | -0.08            | 11        | F          | SPB? / outburst?  |
| 271971626 | HD 62153 AB  | B9IV               | 5214590201474858624 | -0.01          | -0.01            | -         | -          | rot   |
| 276861600 | HD 269777    | B3Ia               | 4661270350708775296 | -1.90          | -0.05            | 5         | F          | SLF   |
| 277022505 | HD 269786    | B1I                | 4657274283151403520 | -3.66          | -0.00            | -         | -          | SLF   |
| 277022967 | HD 37836     | B0e(q)             | 4657280639705552768 | -4.54          | 0.34             | 12/70     | F/X        | rot / SPB? / SLF? / Be                                  |
| 277099925 | HD 269845    | B2.5Ia             | 4661439439319405184 | -2.67          | -0.04            | -         | -          | SLF   |
| 277103567 | HD 37935     | B9.5V              | 4660284883361750912 | -0.48          | -0.04            | 2/30      | F/X        | rot / EV?   |
| 277172980 | HD 37974     | B0.5e              | 4657658356271368064 | -4.36          | 0.51             | 11/6      | F/X        | SLF? / Be   |
| 277173650 | HD 269859    | B1Ia               | 465882353222625920  | -3.23          | -0.16            | 40        | X          | SLF / instr?  |
| 277298891 | Sk-69 237    | B1Ia               | 4657679659311713024 | -1.39          | 0.39             | 1         | F          | SLF   |
| 277982164 | HD 54239     | B9.5/A0III/IV      | 5211241295215037696 | -0.01          | 0.16             | 36        | U          | rot / SPB   |
| 278683664 | HD 47770     | B9.5V              | 548428625513030016  | 0.76           | 0.04             | -         | -          | const??   |
| 278865766 | HD 48971     | B9V                | 5496814662861807360 | 0.46           | -0.02            | -         | -          | const??   |
| 278867172 | HD 49111     | B9.5V              | 5497973449334379904 | 0.96           | -0.04            | -         | -          | const??   |
| 279430029 | HD 53048     | B5/7Vn(e)          | 5484134029618653952 | -1.97          | -0.02            | -         | -          | rot / Be  |
| 279511712 | HD 53921 AB  | B9III+B8V          | 5480486644608749696 | -0.12          | -0.17            | -         | -          | rot   |
| 279957111 | HD 269582    | WN10h              | 4658481718680657792 | -3.51          | 0.33             | 211       | X          | rot   |
| 280051467 | HD 19400 AB  | B8III/IV           | 4645479443883933824 | -0.45          | -0.16            | 1/238     | F/U        | rot   |
| 280684074 | HD 215573    | B6V                | 6351882320090933248 | -0.70          | -0.19            | 1/8       | F/U        | SPB   |

Table 1 continued

Table 1 (continued)

| TIC       | Name        | Sp. Type<br>SIMBAD | Gaia DR2 ID         | $M_G$<br>(mag) | BP - RP<br>(mag) | # Spectra | Instrument | Var. Type                 |
|-----------|-------------|--------------------|---------------------|----------------|------------------|-----------|------------|---------------------------|
| 281703963 | HD 4150 A   | A0IV               | 4908022136034353152 | -0.12          | 0.02             | 1         | F          | hybrid SPB/ $\delta$ Sct  |
| 281741629 | CD-56 152   | Be                 | 4908668373993964032 | -3.05          | -0.23            | 2/6       | F/U        | rot / Be                  |
| 293268667 | HD 47478    | B9V                | 5477090356269215616 | 0.60           | -0.08            | -         | -          | SPB/ rot?                 |
| 293973218 | HD 54967    | B4V                | 5478303942228108288 | -2.08          | -0.21            | -         | -          | rot / SPB                 |
| 294747615 | HD 30612    | B8II/III(pSi)      | 4654833539071572736 | -0.33          | -0.15            | 1         | F          | rot / SLF?                |
| 294872353 | HD 270754   | B1.5Ia             | 4657655435693905408 | -4.36          | -0.02            | 1/20      | F/U        | SLF?                      |
| 300010961 | HD 55478    | B8III              | 5280667689208638976 | -0.00          | -0.14            | -         | -          | rot / $\beta$ Cep ?       |
| 300325379 | HD 58916    | B1.5Ia             | 5281254278662916736 | 0.41           | 0.01             | -         | -          | rot?                      |
| 300329728 | HD 59426    | B9V                | 5267524573886888320 | 0.72           | 0.05             | -         | -          | rot                       |
| 300744369 | HD 63928    | B9V                | 5270696836731782144 | 1.08           | 0.01             | -         | -          | rot                       |
| 300865934 | HD 64484    | B9V                | 5275049837626917504 | 0.04           | -0.06            | -         | -          | instr / outburst?         |
| 306672432 | HD 67252    | B8/9V              | 5271283391825477248 | 0.76           | -0.01            | -         | -          | const? / rot?             |
| 306824672 | HD 68221    | B9V                | 5270992635422817792 | 0.05           | 0.04             | -         | -          | rot? / SPB?               |
| 306829961 | HD 68520 AB | B5III              | 5270986008289935232 | -2.44          | -0.15            | -         | -          | SPB                       |
| 307291308 | HD 71066    | B9/A0IV            | 5221286296008492416 | 0.06           | -0.13            | 13        | U          | instr / rot?              |
| 307291318 | HD 71046 AB | B9III/IV           | 5221286158569529344 | -0.17          | -0.09            | -         | -          | instr / rot?              |
| 307993483 | HD 73990    | B7/8V              | 5221605085661325056 | 0.40           | -0.07            | -         | -          | $\beta$ Cep ? / SPB       |
| 308395911 | HD 66591    | B4V                | 5479669466951012224 | -1.33          | -0.15            | 2         | F          | SPB                       |
| 308454245 | HD 67420    | B9V                | 5275660856854591360 | 0.39           | 0.07             | -         | -          | $\delta$ Sct              |
| 308456810 | HD 67170    | B8III/IV           | 5289613208437434240 | 0.05           | 0.04             | -         | -          | rot?                      |
| 308537791 | HD 67277    | B8III              | 5290024533163062144 | 0.18           | -0.01            | -         | -          | rot                       |
| 308748912 | HD 68423    | B6V                | 5277219758184463488 | -0.74          | -0.06            | -         | -          | SLF? / outburst? / instr  |
| 309702035 | HD 271163   | B3Ia               | 4660142634076536320 | -3.61          | -0.03            | -         | -          | SLF                       |
| 313934087 | HD 224990   | B3/5V              | 2320885329010329216 | -1.32          | -0.19            | 4/18      | F/X        | SPB / rot                 |
| 327856894 | HD 225253   | B8IV/V             | 4701860922688030720 | -0.80          | -0.14            | 3/109     | F/U        | rot? / outburst? / instr? |
| 349829477 | HD 61267    | B9/A0IV            | 5292390815325246976 | 1.07           | 0.09             | -         | -          | const?                    |
| 349907707 | HD 61644    | B5/6IV             | 5289291395127135360 | -0.35          | 0.23             | -         | -          | EB + puls                 |
| 350146577 | HD 63204    | ApSi               | 5288156497263051136 | 0.65           | -0.03            | -         | -          | rot                       |
| 350823719 | HD 41037    | B3V                | 5275962500997316864 | -0.88          | -0.23            | 5/6       | F/U        | SPB? / rot                |
| 354671857 | HD 14228    | B8IV               | 4936685751335824896 | 0.15           | 3.16             | 10/79     | F/U        | SPB? / rot                |

Table 1 continued

Table 1 (continued)

| TIC       | Name                | Sp. Type  | Gaia DR2 ID         | $M_G$<br>(mag) | BP - RP<br>(mag) | # Spectra | Instrument | Var. Type                        |
|-----------|---------------------|-----------|---------------------|----------------|------------------|-----------|------------|----------------------------------|
|           |                     | SIMBAD    |                     |                |                  |           |            |                                  |
| 355141264 | HD 208495           | B9.5V     | 6561093750492347136 | 1.30           | -0.03            | -         | -          | const?                           |
| 355477670 | HD 220802           | B9V       | 6525840590207613824 | 0.34           | -0.09            | 8         | F          | const?                           |
| 355653322 | HD 224686           | B8V       | 6485326438580933888 | -0.74          | -0.07            | 52        | F          | rot? / outburst? / instr?        |
| 358232450 | HD 6882 A           | B6V+B9V   | 4913847589156808960 | 0.10           | -0.18            | 24/33     | F/U        | EB                               |
| 358466708 | CD-60 1931          | B7        | 5290739387520374912 | -0.04          | -0.01            | -         | -          | rot / SPB                        |
| 358467049 | CPD-60 944 AB       | B8pSi     | 5290722929205920640 | 0.18           | 0.06             | -         | -          | rot                              |
| 358467087 | CD-60 1929          | B8.5IV    | 5290722860486442752 | 0.36           | 0.13             | -         | -          | SPB / EV? / rot? / SLF? / instr? |
| 364323837 | HD 40031            | B6III     | 4758153203612698624 | -1.44          | -0.13            | 4         | F          | rot? / SPB?                      |
| 364398190 | CD-60 1978          | B8.5IV-V  | 5290816009737675392 | 0.64           | 0.05             | -         | -          | rot? / SLF?                      |
| 364398342 | HD 66194            | B3Vn      | 4776318613169946624 | -2.36          | -0.33            | 97        | U          | rot? / SPB? / Be                 |
| 364421326 | HD 66109            | B9.5V     | 5287999576341359360 | -0.18          | 0.08             | -         | -          | rot?                             |
| 369457005 | HD 197630           | B8/9V     | 6681797793393053696 | 0.44           | -0.11            | 1/15      | F/U        | rot / SPB?                       |
| 370038084 | HD 26109            | B9.5/A0V  | 4666380781970681472 | 1.65           | 0.19             | -         | -          | const?                           |
| 372913233 | HD 65950            | B8III     | 5290671733195996416 | -1.20          | 0.06             | 5         | F          | const? / outburst? / instr?      |
| 372913582 | CD-60 1954          | B9.5V     | 5290725643625189504 | 0.29           | 0.11             | -         | -          | const? / outburst? / instr?      |
| 372913684 | HD 65987            | B9.5IVpSi | 5290820682661822848 | -0.67          | -0.02            | -         | -          | rot                              |
| 373843852 | HD 269525           | B0I       | 4658678973606061696 | -2.39          | -0.32            | -         | -          | SPB? / rot?                      |
| 389921913 | HD 270196           | B1.5Ia    | 4662413606586588160 | -2.83          | 0.09             | 1/8       | F/U        | SLF                              |
| 391810734 | HD 269655           | B0Ia      | 4661289630893455488 | -2.51          | -0.11            | 2         | F          | SLF                              |
| 391887875 | HD 269660           | B2Ia      | 4657362548954664192 | -3.36          | -0.14            | -         | -          | SLF                              |
| 404768847 | VFTS 533            | B0Ia      | 4651835308326981504 | -1.95          | -0.06            | -         | -          | SPB? / SLF?                      |
| 404768956 | Cl* NGC 2070 Mel 12 | B0.5Ia    | 4658479691454645504 | -2.91          | 0.03             | -         | -          | SLF? / SPB? / instr?             |
| 404796860 | HD 269920           | B3Ia      | 4657652476416109184 | -3.84          | 0.04             | -         | -          | SLF                              |
| 404852071 | Sk-69 265           | B3I       | 4660612881443486720 | -2.93          | -0.09            | -         | -          | SLF                              |
| 404933493 | HD 269997           | B2.5Ia    | 4660135826507549824 | -3.14          | -0.06            | 1         | F          | SLF                              |
| 404967301 | HD 269992           | B2.5Ia    | 4657636675267019008 | -3.51          | 0.18             | 2         | F          | SLF                              |
| 410447919 | HD 64811            | B4III     | -                   | -              | -                | -         | -          | rot/SPB?                         |
| 410451677 | HD 66409            | B8IV/V    | 5290769211774211968 | 0.32           | 0.05             | 4         | F          | rot                              |
| 419065817 | HD 1256             | B6III/IV  | 2364986843479227392 | 0.13           | -0.13            | -         | -          | rot / SPB?                       |
| 425057879 | HD 269676           | O6+O9     | 4651834616802932608 | -1.79          | -0.20            | -         | -          | instr? / binary? / rot?          |

Table 1 continued

Table 1 (*continued*)

| TIC              | Name            | Sp. Type | Gaia DR2 ID         | $M_G$<br>(mag) | BP - RP<br>(mag) | # Spectra | Instrument | Var. Type                         |
|------------------|-----------------|----------|---------------------|----------------|------------------|-----------|------------|-----------------------------------|
| <i>425081475</i> | HD 269700       | B1.5laeq | 4657685534828270976 | -2.78          | 0.33             | 1/48      | F/X        | SLF / rot? / Be                   |
| <i>425083410</i> | HD 269698       | O4Ia     | 4660121743354291328 | -2.38          | -0.34            | 6         | U          | rot / SPB? / SLF?                 |
| <i>425084841</i> | TYC 8891-3638-1 | B1Ia     | 4658474743652257664 | -3.93          | 0.04             | 2/6       | F/U        | SLF                               |
| 441182258        | HD 210934       | B7V      | 6618669608159645312 | -0.53          | -0.14            | -         | -          | instr / SPB/outburst?             |
| 441196602        | HD 211993       | B8/9V    | 6615398767225726848 | 0.46           | -0.09            | 2/9       | U/X        | const.?                           |
| 469906369        | HD 212581 AB    | B9Vn+G0V | 6404338508023617664 | -0.10          | -0.03            | 19        | U          | SPB / $\beta$ Cep / instrumental? |

NOTE—EB = eclipsing binary, EV = ellipsoidal variable, rot = Rotational modulation, SPB,  $\beta$  Cep, SLF = stochastic low-frequency signal, instr = instrumental, const = constant, puls = pulsational signal not clearly identified in any of the previous categories, and  $\delta$  Sct =  $\delta$  Scuti star. We provide an overview of which stars have high-resolution spectra available in the ESO archive. U = UVES, F = FEROS, X = X-SHOOTER, E = ESPRESSO. Stars with TIC numbers in *italics* are LMC members.

## B. TESS LIGHT CURVES AND AMPLITUDE SPECTRA

The light curves and amplitude spectra for the 154 O and B stars considered in this work.

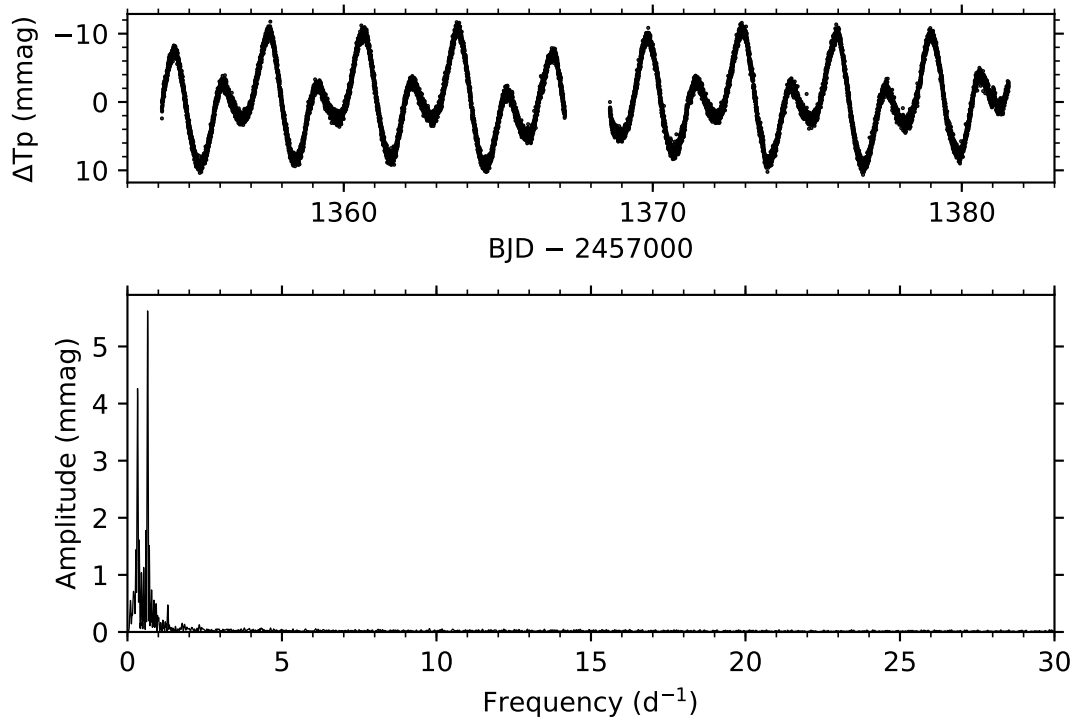


**Figure 4.** The TESS light curve (top) and amplitude spectrum (bottom) of TIC 12359289. The complete figure set (154 images) for all stars considered in this work is available in the online journal.